Environmental Science Nano

The Heterogeneous Diffusion of Polystyrene Nanoparticles and the Effect on the Expression of Quorum-Sensing Genes and EPS Production as a Function of Particle Charge and Biofilm Age.

Journal:	*Environmental Science: Nano*
Manuscript ID	EN-ART-04-2023-000219.R1
Article Type:	Paper

The Heterogeneous Diffusion of Polystyrene Nanoparticles and the Effect on the Expression of Quorum-Sensing Genes and EPS Production as a Function of Particle Charge and Biofilm Age.

Joann M. Rodríguez-Suárez[1*], Anne Gershenson[2], Timothy Umma Onuh[3], Caitlyn S. Butler[1*]

[1]Department of Civil and Environmental Engineering, University of Massachusetts Amherst, Amherst MA 01003

[2]Department of Biochemistry and Molecular Biology, University of Massachusetts Amherst, Amherst MA 01003

[3]Department of Chemical Engineering, University of Massachusetts Amherst, Amherst MA 01003

[*]Correspondence: Caitlyn S. Butler and Joann M. Rodríguez-Suárez

E-mail: csbutler@engin.umass.edu and joan.rodriguez8@upr.edu

ABSTRACT

Biofilms are abundantly present in both natural and engineered environmental systems and will likely influence broader particle fate and transport phenomena. While some developed models describe the interactions between nanoparticles and biofilms, studies are only beginning to uncover the complexity of nanoparticle diffusion patterns. With the knowledge of the nanoparticle potential to influence bacterial processes, more systematic studies are needed to uncover the dynamics of bacteria-nanoparticle interactions. This study explored specific microbial responses to nanoparticles and the heterogeneity of nanoparticle diffusion. *Pseudomonas aeruginosa* biofilms (cultivated for 48 and 96 hours, representing early and late stages of development) were exposed to charged (aminated and carboxylated) polystyrene nanoparticles. With a combination of advanced fluorescence microscopy and real time quantitative PCR, we characterized the diffusion of polystyrene nanoparticles in *P. aeruginosa* biofilms and evaluated how biofilms respond to the presence of nanoparticles in terms of the expression of key EPS production-associated genes (*pelA* and *rpsL*) and quorum-sensing associated (*lasR*) genes. Our findings show that nanoparticle diffusion coefficients are independent of the particle surface charge only in mature biofilms and that the presence of nanoparticles influences bacterial gene expression. Independent of the particle's charge polystyrene nanoparticles down-regulated *pelA* in mature biofilms. By contrast, charge-specific responses were identified in *lasR* and *rpsL* gene expression. The targeted genes expression analysis and heterogeneous diffusion models demonstrate that particle charge influences nanoparticle mobility and provides significant insight into the intrinsic structural heterogeneity of *P. aeruginosa* biofilms. These findings suggest that biofilm maturity and particle charge are

essential factors to consider when evaluating the transport of nanoparticles within a biofilm matrix.

ENVIRONMENTAL SIGNIFICANCE

Engineered nanoparticles are a growing environmental concern, and their fate and transport in natural and engineered systems are not yet fully understood. Biofilms in environmental and engineered systems play a role in determining nanoparticle fate and transport. Herein, we present a study to explore the complexity of nanoparticle diffusion and their influence on biofilm responses. The findings demonstrate that heterogenous transport of polystyrene nanoparticles that varies by charge can also uniquely influence bacterial gene expression of quorum-sensing systems and protein expression, as well as nanoparticle mobility. These insights provide a deeper understanding of the heterogeneity of nanoparticle behavior in biofilms and highlight the need for more systematic studies to better identify the environmental impact of nanoparticles.

INTRODUCTION

The field of nanotechnology has seen an exponential growth in recent years, with nanoparticles (NPs) being increasingly utilized in various industrial and commercial applications such as medicine, electronics, agriculture, energy and transportation (1–4). However, the release of these nanoparticles into the environment has the potential to disrupt ecosystem stability (5). In recent years, studies have demonstrated that nanoparticles can exhibit toxicity to cells (6,7). One class of nanoparticles that has garnered significant attention is polystyrene NPs (8). There is a particular need to further investigate the effects of polystyrene NPs and others on biological systems because studies have shown that these particles persist and interact with microorganisms in the environment (9,10).

Bacteria in the environment live and grow in highly organized communities called biofilms that are usually associated with biological or non-biological surfaces (11–13). Biofilms are complex structures of microorganisms embedded in a heterogeneous matrix of macromolecules, well known as extracellular polymeric substances (EPS) (14,15). Although, the EPS serve as a physical barrier that embeds and shields the microbial cells, studies have shown that the EPS can influence the penetration of external agents into the biofilm, including nanoparticles and constrain their motion (16–18). And, bacteria found in biofilms can regulate the EPS properties through gene expression at different stages of biofilm development and maturity. Given that biofilms have been found to be nanoparticle reservoirs (19), exposure of biofilms to NPs may have significant effects on the viability of microbes as well as the biofilm structure (7).

In natural biofilms, which are dynamic and active, the microbial habitat and the biofilm structure interact in a responsive manner. Therefore, the effects of NPs on cellular responses depend not only on the metabolic capabilities and cell membrane properties of the microbe but also on the physical and chemical properties of the NPs (20,21). For example, inorganic nanoparticles (e.g., titanium dioxide, silver, cadmium oxide and zero valent iron) can generate reactive oxygen species (ROS) that can activate death signaling pathways, survival signaling mechanisms, and affect gene expression (22–26). In addition, NPs can affect cell-cell communication by altering the expression of quorum sensing (QS) systems that are vital for biofilm formation and maturation (27). The QS systems work through receptors in the membrane that bind the extracellular signal and then interact with response regulators to modify transcriptional levels and regulate cooperative behaviors (28). Furthermore, these QS signaling networks can regulate the EPS secreted by the bacterial cells as a response to environmental stimuli (29). Our hypothesis is that heterogeneous diffusion of NPs influences how NPs accumulate in biofilms.

NPs are a known stressor for the cells and cause changes (increases or decreases) in the genetic expression of key EPS production and quorum-sensing systems. If NPs are stressors for the bacteria and lead to changes in the production of EPS components and quorum sensing signals, the EPS matrix composition can change resulting in a change in biofilm properties and a heterogenous diffusion.

The specific objective of this study was to characterize the diffusion of cationic and anionic polystyrene NPs in *Pseudomonas aeruginosa* biofilms and evaluate the bacterial response to the NP's presence in order to provide a window into the complex interplay between nanoparticles, microbial transcription, and biofilm architecture. Specifically, (1) to characterize the diffusion of polystyrene nanoparticles in *Pseudomonas aeruginosa* biofilms as a function of particle charge, (2) to identify the role of biofilm maturity in the diffusion coefficients and diffusive mode of the nanoparticles and, (3) assess the role of biofilm age in the magnitude of the cellular response to cationic and anionic polystyrene NP exposure by identifying changes in the expression of genes related to polysaccharide biosynthesis and quorum sensing systems.

EXPERIMENTAL

For this experiment, we used the bacteria *Pseudomonas aeruginosa,* strain PAO1 *ΔwspF Δpsl* P_{BAD}*pel*. This *P. aeruginosa* strain was obtained from the Parsek Lab at the University of Washington in 2019 and culture has been maintain in glycerol in –80 °C storage. The strain possesses *wspF*, nonpolar mutation; *pslBCD*, polar mutant of the *psl* operon; arabinose-inducible *pel* operon and is described in Jennings et al., 2015 (30). The PAO1 *ΔwspF Δpsl PBADpel* strain have only the polysaccharide *Pel* as the primary matrix structural polysaccharide, making it suitable to study the effect of the NPs on polysaccharide production. The bacteria were cultivated

in liquid Jensen's media (30) overnight at 37° C with slow mixing and then diluted to an optical density OD_{600} of 0.05. Jensen's media contains NaCl (85.6 mM), K_2HPO_4 (14.4 mM), ammonium sulfate (15.1 mM), glucose (0.3 mM), 0.5% (vol/vol) arabinose, $MgSO_4$ (1.33 mM), $CaCl_2$ (0.14 mM), $FeSO_4$ (0.0039 mM) and $ZnSO_4$ (0.0085 mM) and pH adjusted to 7.14 to promote biofilm formation as described in Jennings et al. (30). In order to observe the samples under the microscope without disturbing the biofilm structure in a flow cell chamber, flow cell chambers (512 µL) were custom designed, and 3D printed. The flow cell body was made of the polymer PA 2200 and the chambers were closed with glass cover slips of 0.17 mm thickness with dimensions of 22 mm x 22 mm. After the bacterial inoculum was added to the flow cell chambers, the cells were allowed to attach to the glass coverslip substratum for 3 hours before starting the media flow of 30 mL/hour through the chambers. Biofilms were grown for 48 and 96 hours in a controlled temperature room at 37°C with a constant flow of Jensen's minimal glucose fresh media to promote biofilm formation and maintain optimal pH (30–32). Times selected were based on biofilm growth in the flow cells. Growth profiles with this *P. aeruginosa* isolate in these flow cells was determined by replicate, time-based, destructive sampling of flow cells and quantifying 16S rRNA gene copies. The 48-hr time marks the end of the exponential phase of growth and the 96-hr time represents a maturation through growth stabilization, well before evidence of decay. Additionally, Dynamic light scattering (DLS) Malvern Zetasizer NS (Worcestershire, U.K.) was used to measure the zeta potential and hydrodynamic diameter of the P. aeruginosa cells and the NPs individually and in NP-cells samples.

To evaluate if NP accumulation in the biofilms stressed bacteria and affected gene expression of key EPS production and quorum sensing systems, we exposed the biofilms in the flow cells to cationic and anionic nanoparticles 1mM 4-(2-hydroxyethyl)-1-piperazineethanesulfonic acid

(HEPES), pH=7.3, for 6 hours. Biofilms were cultivated for 48 and 96 hours in 3 flow cells for a total of 9 chambers with biofilm replicates with constant flow of Jensen media. When the biofilms reached the desired maturation, the chambers were washed with 5 mL of 1 mM HEPES buffer (pH 7.3) in order to remove all of the liquid media and suspended biomass in the chamber that could cause the NPs to aggregate. Two of the flow cells were treated with cationic or anionic polystyrene NPs in 1 mM HEPES buffer and the other one was treated with just 1 mM HEPES buffer as a control. The approximate NP concentration added to each sample was 3.0×10^7 particles per sample. The cationic NPs were positively charged fluorescent aminated polystyrene beads (Invitrogen FluoSpheres, max abs/em: 580/605 and diameter, d = 64 ± 3.4 nm) and the anionic NPs were negatively charged fluorescent carboxylated polystyrene beads (Invitrogen FluoSpheres, max abs/em: 580/605 and d = 63 ± 3.1 nm). After 6 hours of exposure to the NPs under static conditions, the flow cells were opened, and samples were collected for further extractions. Biofilms from each cell were scraped with sterile pipette tip using an identical swabbing pattern for each flow cell area to minimize collection biases. The collected biomass was resuspended in 100 μL phosphate buffer for protein, eDNA, RNA, and polysaccharide extraction 138 procedures that are described in subsequent sections. For intact biofilms, microscopy data were recorded after 6 hours of biofilm exposure to the NPs under static conditions. The experiment was repeated twice for each biofilm age (Results from experiment 1 are reported in the main text and results for experiment 2 are reported in the Supplementary Information)

Microscopic data acquisition

The samples were observed, without opening the flow cells or disturbing the biofilm, using the Nikon CrestV2 Spinning disk confocal microscope with a sCMOS Prime 95B camera. This microscope setup allows the use of a low-light technique appropriate for live cells imaging. For each biofilm sample, 6,000 frames of data were collected at a rate of 100 frames/s using an Apo TIRF 100x NA 1.49 objective at the point along the z axis (perpendicular to the flow cells) where the fluorescence from the NPs was first observed ($z = 4500 \pm 703$ μm, relative to the coverslip). The red fluorescent NPs were excited with a 561 nm laser and a laser power of 38 mW (50% of the maximum, 75 mW, fiber output for 561 nm), for both, the aminated and carboxylated modified polystyrene nanoparticles. For each sample three randomly-selected but distributed (top, middle, and bottom of the sample area) fields of view of 256 x 256 pixels (0.11 μm/pixel) were recorded to collect images from different biofilm locations. The samples from the control, no NPs + flow cell, was observed to account for any background fluorescence. Table 2 shows the average number of particles tracked within each field for both independent experiments.

Microscopy data analysis

To characterize NP diffusion and the structural features of 48 and 96 hours PAO1 *ΔwspF Δpsl* P_{BAD}*pel* biofilms, the microscopic images were analyzed using correlation analysis and single particle tracking. Two-dimensional pair correlation function (2D-pCF) was used to generate connectivity maps. 2D-pCF is an appropriate method to visualize features of the biofilm matrix that require high spatial resolution (e.g., barriers for NP diffusion) because it does not rely on a spatial average. The analysis was performed using a pCF pixel distance of 4, detecting temporally and spatially correlating fluorescence at a random adjacent location at a maximum

distance of 0.44 μm (4 pixels) away. For the connectivity maps, the arrow length (line length) selected was 5 pixels (0.55 μm). The ratio of void to non-void space within the connectivity maps was determined using ImageJ by binarizing the image to black and white and quantifying the number of pixels in the void and non-void spaces, respectively. The mean void to non-void ratio for each experimental condition was calculated using all three fields of view from both experiments (N=6).

Single particle tracking (SPT) was used to analyze individual tracks of the NPs moving through the biofilm and to perform a particle count. The SPT analysis was done using the algorithm in the NIS-Elements software (Nikon's universal software platform) (33). For this study, a random motion model was selected, and it allowed gaps in tracks of a maximum size of 10 frames based on the average time a particle stayed visible in the microscopic images. All trajectories longer than 50 frames were selected; shorter tracks were not considered in the analysis.

For the identification and visualization of the spatial distribution of diffusion modes and NP diffusion coefficients (*D*), an image Mean Square Displacement (iMSD) analysis was performed. One of the advantages of using iMSD, is that it is based on the calculation of mean square displacements (MSD) allowing the visualization of the distribution of diffusion coefficients in the form of maps (34). The iMSD method was used to identify and visualize the spatial distribution of diffusion modes and the diffusion coefficients (*D*) of NPs moving in the 48 and 96 hr old biofilm samples. For the iMSD analysis, a region of interest (ROI) of 32 x 32 pixel and a moving window with an ROI overlap of 1⁄4 (8 X 8 pixels) was selected. The data were analyzed using the "all models" option for diffusion (free diffusion, confined, and partially confined) because a wide variety of diffusion behaviors was observed in the microscopic images.

RNA extraction and real-time quantitative PCR experiment

After the biofilm samples were collected as described above, the samples were centrifuged (10,000 rpm for 5 minutes at room temperature) in order to separate the bacterial cells from the loosely bound extracellular polymeric substances (EPS). The supernatant part of the sample was used to extract and quantify the production of extracellular DNA, and the cell pellet was used for RNA extraction. The RNA extraction procedure was performed immediately after sample collection using the QIAamp Viral RNA extraction kit from QIAGEN following the manufacturer's recommended protocol (note that despite its name, this kit includes directions for isolating RNA from cell cultures). RNA concentrations were measured using the Qubit RNA HS Assay kit from Invitrogen with the Qubit Fluorometer. The messenger RNA (mRNA) was then converted to single stranded complementary DNA (cDNA) suitable for the quantitative polymeric chain reaction (qPCR) with reverse transcriptase using the High-Capacity cDNA Reverse Transcription kit from Applied Biosystems. To synthesize cDNA from the RNA, we followed the protocol recommended by the manufacturer. In brief, the reverse transcription master mix was prepared by adding the recommended amounts of 10X RT buffer, 25X dNTP mix, 10X RT random primers, the MultiScribe reverse transcriptase and the necessary nuclease-free water for a total reaction volume of 10 µL. In a 600 µL microtube, the master mix was mixed with 10 µL of the RNA sample and the reverse transcription reaction was performed in a thermal cycler following 3 steps, 25° C for 10 min, 37° C for 120 min and ending with 5 min at 85° C. The resulting cDNA concentration was quantified using the Qubit dsDNA HS Assay kit from Invitrogen with the Qubit Fluorometer.

The effects of cationic and anionic polystyrene NPs on the expression of genes related to polysaccharide production and quorum sensing systems was assessed through qPCR experiments

performed for both biofilm ages (48 and 96 hours). The expression of genes related to polysaccharide production was assessed using primers for the *pelA* gene (32). To evaluate the effect of the NP's presence on the expression of genes related to the quorum sensing system, we used specific primers for *lasR* (28,32). *LasR* and *rhlR* are the most well-known *P. aeruginosa* quorum sensing systems that control virulence factor production, swarming motility and biofilm development and maturation (28). The genes *ampR* (ampicillin resistant gene) and *rpsL* (encodes the ribosomal S12 protein) were used as the reference transcripts (32,35). Table 1 summarizes the forward and reverse sequences of all the primers used.

Amplification of the cDNA templates was done with a StepOne Real Time PCR System from Applied Biosystems using iTaq Universal SYBR Green Supermix from BIORAD for dye-based detection. For each PCR reaction, 2 µL of cDNA template, 10 µL of 2X master mix, 1.8 µL of the reverse and forward primer (final concentration 450 nM) and 6.2 µL of RNase free water for a total reaction volume of 20 µL was used. The real-time PCR conditions for the amplification of 16S rDNA gene were 600 s at 95 °C followed by 40 cycles: 15 s at 95 °C for denaturation, 60 s at 60 °C for annealing. One last gradient step from 60 to 95 °C with an increase of 0.3 °C/s was added to obtain a melting curve. The qPCR reaction conditions were an initial activation cycle of 600 s at 95 °C, followed by 35 cycles of 10 s at 95 °C for denaturation and 60 s at a specific temperature for annealing/extension of 60.0°C for *pelA, lasR, ampR* and *rpsL.* A melting curve analysis was performed using a temperature gradient of 60 °C to 95 °C at 0.3 °C/s intervals to verify the specific amplification of a single PCR product. Each plate run for each gene target included triplicates of non-template control (wells without the cDNA template), 3 biological replicates with two technical replicates for each condition (control biofilm, aminated NP treated biofilm and carboxylated NP treated biofilm, N=6 for each) and standard samples to generate

standard curves for the PCR efficiency estimation. Different genes were analyzed in different runs.

The qPCR data was analyzed using relative quantification(36). The gene of interest (*pelA, lasR,* or *rpsL*) was compared to the reference gene (*ampR*) to normalize the changes for each sample using the reaction efficiencies for each run calculated from the standard curves (for each gene, target and reference) using the following equation:

$$Efficiency = 10^{\,slope} - 1 \qquad (1)$$

Using the mean quantitative cycle (C_q) of the technical replicates for each biological replicate of the control sample and the NP treated sample, the normalized fold expression of target genes was calculated using the following equation:

$$Normalized\ fold\ expression = Log_2\left(\frac{(E_{target})^{\Delta C_{q\ target}}}{(E_{ref})^{\Delta C_{q\ ref}}}\right) \qquad (2)$$

This equation considers the efficiency for the reference gene (E_{ref}) and the efficiency for the gene target (E_{target}).

Protein and eDNA quantification

The total protein concentration in each sample fraction, unbound proteins from the sample supernatant and bound and intracellular proteins from the cell pellet, were measured using the Qubit Protein Assay Kit with the Qubit Fluorometer using bovine serum albumin (BSA) as the standard.

Extracellular DNA (eDNA) was extracted from the supernatant portion of the biofilm samples to avoid contamination with genomic DNA from inside the cells using the DNeasy® PowerSoil Pro Kit from QIAGEN following the manufacturer protocol. The extracted eDNA was quantified using the Qubit dsDNA HS Assay kit. We used the eDNA concentration from the "Control" as a reference sample to determine if there was an increase or decrease in eDNA secretion due to the presence of NPs.

Statistical Analysis

The statistical analysis comparing the difference between the histograms of diffusion coefficients obtained by the iMSD analysis was performed in R using the permutation test of symmetry where the levels of the various conditions were treated as having paired or repeated data. Kernel (Scott) probability density estimates of the diffusion coefficient (D) distributions were used. If the p- value was lower than 0.05 then the null hypothesis that there was no difference between the distributions was rejected. In this data, N varied depending on the histogram but $N > 100$ for all conditions.

For statistical comparisons between the control and the NP treated samples in terms of the normalized fold expression of the *pelA, lasR,* and *rpsL* genes and the total protein concentration, a T-test was run in Minitab 19, using the average value and standard deviation of all three biological replicates from the two independent experiments (N=6 for each sample).

RESULTS AND DISCUSSION

Aminated and carboxylated nanoparticles can bind to EPS components in biofilms

After 6 hours of exposure to aminated and carboxylated polystyrene NPs, the biofilm samples

were observed under the Nikon CrestV2 Spinning disk confocal microscope. The samples from the control (no NPs) flow cell, were observed to quantify any background fluorescence from the biofilm. No significant fluorescence emission was detected in the biofilm only control samples for 561 nm wavelength excitation. The number of particles in the field of view was lower for biofilm samples with aminated NPs compared to biofilm samples with carboxylated NPs. The average number of particles obtained from a single particle tracking (SPT) analysis are presented in Table 2. Similar trends were found in Experiments 1 and 2, however, more NPs (aminated and carboxylated) were detected in Experiment 2 (Experiment 2 results are included in the Supplementary Information). Particle aggregation or possible NP binding to biofilm components was observed in all of the 48 hr and 96 hr biofilm samples in the microscopy images (Figure S3).

Before adding the NP solution to the flow cell chamber, a wash step was performed to reduce aggregation of the NPs due to the cultivation media. If the wash step was effective removing the liquid media in the chamber, it is possible that the carboxylated and aminated NPs bound to biofilm components due to electrostatic attraction. In the case of the PAO1 *ΔwspF Δpsl* P_{BAD}*pel* strain, the biofilm matrix contains negatively charged components (e.g., eDNA) as well as positively charged polysaccharides (e.g., *Pel*). In 1 mM HEPES (pH = 7.14) at 37° C the aminated polystyrene NPs and the carboxylated polystyrene NPs have zeta potentials of +25 ± 3.3 mV and -34 ± 3.1 mV. Birjiniuk et al. (14) previously identified a strong dependence between carboxylated NP mobility in biofilms and NP interactions with charged portions of the EPS. PAO1 *ΔwspF Δpsl* P_{BAD}*pel* is a *Pel* overproducer strain when cultivated with the arabinose inducer (37) and attractive forces between the cationic exopolysaccharide *Pel* and the carboxylated NPs are expected (30). This probable attraction likely explains the apparent binding of carboxylated NPs to the biofilm matrix. An electrostatic potential between the NPs and

bacterial cells (PAO1 *ΔwspF Δpsl* P_{BAD}*pel* cells in 1 mM HEPES (pH 7.14)) has a zeta potential of -26 ± 1.7 mV. The association of NP and *P. aerugino*sa may also be explained by an observed increase in average cell size as was observed when suspended cells were exposed to aminated NPs (from 520 ± 150 nm to 1,100 ± 380 nm) as measured using dynamic light scattering (DLS) (Malvern Zetasizer NS,Worcestershire, U.K.) (Figure S3)

It is generally known that when a nanoparticle enters a biological matrix, it nearly instantly acquires a corona over its surface in either monolayer or multilayer form (5,11). Studies have shown that surface modification of NPs plays a critical role in corona formation and thus, in NP – biofilm interactions (17). Nervius et al. (38) showed that charge and size are important in modulating corona composition and the transport of fluorescent polystyrene NPs in *Alteromonas macleodii* biofilms where surface sulfate (SO_4^-) groups on polystyrene NPs resulted in greater sorption compared to NPs functionalized with amine (–NH) or carboxyl groups. In the *P. aeruginosa* biofilm model used in the present study, eDNA and pel have been shown to be key structural features (30). As eDNA and pel possess a polyanionic nature, in the case of polystyrene NPs that are coated with positive and negatively charged molecules, electrostatic interactions can play a primary role (39) but not the only role in governing interactions between NPs and the *P. aeruginosa* matrix. Zajac et al. (40) demonstrated in biofilms, that the interactions of polystrene NPs with the cell membranes of *Staphylococcus aureus* and *Klebsiella pneumoniae* led to changes in the zeta-potential of the bacterial cells, without causing cell death, and outcomes were dependent on particle concentration, pH, and exposure time. Additionally, studies have showed that kinetics of the interactions between biofilm components and functionalized nanoparticles were influenced by hydrophobic forces, van der Waals forces, pH, and steric hindrance (11,41,42). However, in *P. aeruginosa biofilms*, electrostatic interactions were found to dominate over van der Waals forces,

hydrophobic interactions, and hydrogen bonding (43,44). We, therefore, highlight on the potential role of electrostatic interaction in our studies of NP diffusion and interactions in *P. aeruginosa* biofilms. In this study, we acknowledge the diverse complex interplay of factors influencing the fate of nanoparticle transport in biofilms. However, this study investigate the overall behavior of nanoparticle diffusion within biofilms, rather than examining the individual effects of these interactions on nanoparticle diffusion.

Nanoparticle diffusion in biofilms depends on biofilm maturity and particle charge

The connectivity maps, which illustrate the space in the biofilm network that the NPs are able to access (biofilm voids), are presented in Figure 1 and for experiment 2, Figure S4. In a previous study of NP diffusion in a model alginate matrix, we identified clear differences in the areas NPs were able to access in a heterogeneous polymeric matrix due to the differences in particle size (15). In this study the particles have similar sizes (d_{NH3+} = 64 ± 3.4 nm and d_{COOH-} = 63 ± 3.1 nm), though we considered both positively and negatively charge the functional groups at the particle surface.

There are no clear qualitative differences in the connectivity maps suggesting that the particle charge does not strongly influence the shape and size of the areas the NPs can access. Within the images for each condition, the connectivity maps show different void shapes and sizes likely indicating the heterogeneity of the void spaces in these bacterial biofilms. Quantifying the ratio of void to non-void space in the images does reveal small differences in the average ratio between connectivity maps by age but less so for surface functional group for the 48 hr biofilms (0.17 ± 0.08 – carboxylated NPs, 0.12 ± 0.03 – aminated NPs) and the 96 hr biofilm (0.07 ± 0.04 – carboxylated NPs, 0.10 ± 0.07 – aminated NPs). Anisotropy determined from iMSD analysis

for each condition indicates reduction in the average anisotropy by age and particle charge for carboxylated (0.14 ± 0.08 for 48 hours and 0.06 ± 0.01 for 96 hours) and aminated NPs (0.08 ± 0.04 for 48 hours and 0.04 ± 0.01 for 96 hr) . Together this could mean biofilm ages chosen for this study have some influence on reduced void accessibility for the 63-64 nm particles and to a lesser extent both biofilm age and particle charge influence anisotropy.

The diffusion of aminated and carboxylated NPs in PAO1 *ΔwspF Δpsl* P_{BAD}*pel* was characterized in terms of diffusion coefficients (*D*) and the visual maps of *D* revealed spatial variability in NP diffusion coefficients throughout the biofilm network (Figure 2, Experiment 2 – Figure S5). The overall behavior of the aminated and carboxylated nanoparticles in Experiments 1 and 2 were similar, the *D* for aminated NPs in 48 hr biofilms samples were lower (p-value $_{Exp1}$= 0.003, p-value $_{Exp2}$= 0.001) than the *D* for the carboxylated NPs and similar diffusion coefficients were calculated for both types of NPs diffusing in 96 hr biofilm samples (p-value $_{Exp1}$ = 0.866, p-value $_{Exp2}$ = 0.146). These results concur with a previous study of NPs diffusing in 2 day old *Escherichia coli* biofilms, where the carboxylated NPs were more mobile than aminated NPs (14). The observation that anionic particles have similar diffusion coefficients to cationic particles in 96 hr biofilms could be due to cationic and anionic patches formed by EPS components at the nanoscale which may be more abundant in more mature biofilms (19). The average diffusion coefficient, *D,* were not exactly reproduced for both experimental replicates, agreeing with previous experiments that have identified variability in biofilms produced from the same monoculture (12). However, when comparing the *D* distributions between samples from Experiment 1 and 2, there was no statistical difference (all p-value between samples replicates were > 0.05). The use of distributions instead of average values to characterize NP diffusion and compare biofilm replicates highlights the intrinsic heterogeneity (microdomains) of the biofilm

matrix. Moving towards using distributions of *D* instead of effective *D* values to compare results from diffusion studies in heterogeneous matrices (under similar conditions) could reduce the discrepancies between *D* values in biofilm replicates that researchers have previously reported (12).

Peulen & Wilkinson (12) studied the diffusion of carboxylated polystyrene 57 nm NPs in 9-15 hr old biofilms of *P. fluorescence* under static conditions using fluorescence correlation spectroscopy. The calculated *D* was higher (D = 5.4 $\mu m^2/s$) compared to the values we obtained in this study (D = 0.31 - 0.68 $\mu m^2/s$), but this could be due to the differences in bacterial strain, time of NP exposure, biofilm age and cultivation conditions which are all factors that can affect biofilm physicochemical properties. The diffusion coefficient values for the caboxylated polystyrene NPs in this study are lower than the values obtained in previous studies for 20 nm and 100 nm particles with similar chemical composition diffusing in alginate but greater than the diffusion coefficients calculated for 200 nm NPs in alginate (15). In bacterial biofilms, it is reasonable to have lower *D* values than in a single component polymeric matrix due to the interactions between EPS components (proteins, nucleic acids, lipids and polysaccharides) that affect the viscosity, pseudoplasticity and elasticity of the matrix (45) and restrict NP mobility.

Nanoparticles can display different diffusion modes in biofilm matrices

When NPs diffuse in a biofilm heterogeneous matrix, NPs can be freely diffusing, confined by the biofilm matrix or confined for a period of time before resuming free diffusion, so-called partial confinement. From the iMSD analysis, maps of diffusion modes were obtained and presented in Figure 3 and Figure S7 for the second experiment.. In both experiments, the

proportion of freely diffusing particles (blue) increased for aminated NPs in 96 hr biofilms, but decreased for carboxylated NPs, albeit the magnitude of change is different for each experiment. Similarly, the percent of the maps showing confinement (yellow) increased for the carboxylated NPs but decreased for the aminated particles in the 96 hour biofilms. These results are consistent with the diffusion coefficient presented in Figure 2 where the *D* of the carboxylated NPs decrease in mature biofilms compared to the *D* in younger 48 hr biofilms and the *D* values increase for the aminated NPs in the 96 hr biofilms (mature).

Though freely diffusing (blue) and confined (yellow) trends are consistently increasing or decreasing across the two experimental sets, there are some differences in the magnitudes of these observations that influences what portion of particles experience transitional mode of partially confinement (red). In the case of the carboxylated NPs, the *D* for NP diffusion in the 48 hr biofilms was lower in Experiment 2 compared to Experiment 1 ($D_{Exp1} = 0.68 \pm 1.28$ $\mu m^2/s$ and $D_{Exp2} = 0.41 \pm 0.53$ $\mu m^2/s$, p-value= 0.0003). These differences between experimental replicates emphasizes the variability that biofilms can have even when formed in similar, well-controlled conditions and by the same microorganism. The trends are consistent, but magnitudes of changes varied in this experimental because of the native heterogeneity in the biofilm matrix. In addition, these results suggest that even in matrices where the NPs have similar average diffusion coefficients, the modes of diffusion could be different.

Changes in the diffusion modes between biofilms as a function of age could be related to the possible binding of the NPs to the biofilm components which are more abundant in the more mature biofilms. This hitchhiking mechanism, presented previously as the mobility of the bound complex, can make NP movement dependent on the movement of cells and other components of the biofilm matrix. In other words, if a particle is bound to a biofilm component that is itself

diffusing, then the particle will be taken along with that component's translational motion (46). If the cationic particles are for example, bound to the PAO1 *ΔwspF Δpsl* P_{BAD}*pel* cells, then the NP diffusion could be slowed down because the cells move more slowly than the NPs. In a previous study of single microcolony diffusion in *P. aeruginosa* biofilms, the diffusion coefficients depended on the microcolony size and were close to the values obtained in the biofilm samples from this study, for larger microcolonies $D = 0.28 \pm 0.12$ $\mu m^2/s$ and for smaller ones, $D = 0.49 \pm 0.25$ $\mu m^2/s$(47).

If the NP is bound to a polymer, then the degree of crosslinking (DCL) of the polymer could influence the overall NP diffusion coefficient (*D*). If carboxylated NPs were to bind to the cationic polysaccharide (*Pel*) produced by PAO1 *ΔwspF Δpsl* P_{BAD}*pel,* this could explain why the areas of confinement increased in the 96 hr biofilm samples. Polymers with lower DCL that are weakly physically cross-linked and flexible will allow faster polymer dynamics which might increase the probability of escape from confinement.(48) In this case, the observed increase in the proportion of confined or partially confined carboxylated NPs could arise from an increase in the *Pel* DCL due to biofilm maturity.

Peulen & Wilkinson (12), concluded that considering only biofilm viscosity and tortuosity is not enough to accurately describe the diffusion of NPs in biofilms. As mentioned before, if NPs get attached to cells or other biofilms components the dynamic movement of these components can alter the diffusion of the NP and decrease the *D* of the NPs. In terms of the EPS architecture, the NPs may be able to reach areas of the biofilm that bacterial sized particles (> 500 nm) would not be able to reach. In this study, the tracks of NP motion were obtained from the SPT analysis and are presented as polar graphs in Figure 4.

The tracks for the aminated NPs in the 48 hr biofilm samples are short and overlapping. Though in the 96 hr biofilms, the tracks are longer with less overlap, and paths have more random patterns of movement. In the case of the carboxylated NPs, in 48 hr biofilm samples the tracks are longer and non-directional, but in the 96 hr samples the tracks are shorter, thicker and have a variety of patterns. A twisting pattern have been previously identified in holographic 3D tracking of *P. aeruginosa* cells swimming behaviors (49). To elucidate how the movement of the NPs that can bind to cells might be affected by cellular movement, further experiments (for example simultaneously tracking fluorescently labeled bacteria and NPs) that allow direct comparisons between cell and fluorescent particle motion would be useful.

Polystyrene nanoparticles affected gene expression

We explored the impact of cationic and anionic polystyrene nanoparticles (NPs) (d=64 and 63 nm, respectively) on the expression of *pelA, lasR and rpsL* transcripts using qPCR. Figure 5 shows the normalized fold expression of the genes of interest for each condition. *Pel* is a cationic exopolysaccharide that provides the primary structural scaffold for *P. aeruginosa* biofilms especially for the surface-attached submerged biofilms cultivated in flow cells. *Pel* is also important for initiating and maintaining cell to cell interactions for cell attachment to the surface (30,32,50). An increase in polysaccharide concentration could increase the degree of cross-linking (DCL) between EPS components, which may restrict diffusion processes in the matrix (15). In the younger biofilms (48 hr) samples, no statistically significant changes were identified between the unexposed biofilms and the NP treated biofilm samples. However, in the older biofilms (96 hr), the *pelA* transcripts produced by untreated biofilms were significantly higher than the NP treated samples (p-value $_{NH3+}$ = 0.03 and p-value $_{COOH-}$ =0.04). These results suggest that aminated and carboxylated polystyrene nanoparticles are effective in down- regulating *pelA*

independent of particle surface functionalization. It has been proposed that the *Pel A* protein is located in the periplasm and is related to polymer (*Pel*) chain length regulation. However, it is not clear if a decrease in the expression of the *pelA* gene would lead to a decrease in the overall *Pel* production (in terms of concentration) or if only the polymer chain length would be affected (39,51). Further experiments can focus on evaluating the effects on the biofilm composition due to the downregulation of *pelA* by cationic and anionic NP in mature biofilms using extraction and analytical methods to quantify *Pel* (30). According to our results, polystyrene NPs may not affect the initial stages of PAO1 *ΔwspF Δpsl* P_{BAD}*pel* transcription of *Pel* associated genes independent of the particle surface properties. However, cells in mature biofilms may be threatened by aminated and carboxylated modified polystyrene NPs as shown by the decrease in *pelA* transcriptomes after NP exposure. As shown in previous studies of *Pel* mutants (50), in addition to EPS biosynthesis *Pel* genes are also required for the formation of carbohydrate-containing compounds that encase the bacterial cells. A decrease in polysaccharides production due to the presence of polystyrene NPs could disrupt the carbohydrate layer encasing the bacteria resulting in an increase in susceptibility to antibiotics. In a previous study, it was found that for *P. aeruginosa* strains PAO1 and PA14 in biofilms *Pel* protects the bacteria from the antibiotic tobramycin (32). The decrease in *pelA* transcripts after NP (aminated and carboxylated) exposure could have implications in efforts towards biofilm control depending on the *P. aeruginosa* strain. For the case of the PAO1 strain, the reduction in *Pel* doesn't affect the growth of the biofilm but in other *P. aeruginosa* strains (e.g., PA14) decreases in *Pel* production can prohibit the biofilms from growing larger (32). However, further studies are needed to test these hypotheses, for example, studies to measure *Pel* production and biofilm growth (e.g., biofilm thickness and dispersion) after NP exposure.

In addition to the effect of aminated and carboxylated polystyrene NPs on the expression of *pelA* we evaluated their effects on the expression of *lasR*. *LasR* is one of most well-known quorum-sensing systems of *P. aeruginosa* that controls virulence factor production, swarming motility, and biofilm maturation. Bacterial cell density is monitored by signaling molecules, in the case of *P. aeruginosa*, the homoserine lactones (HSLs). At a certain cell density, *lasR* responds to an increase in biomass and the cells disperse from the biofilm through the quorum-sensing influence. The results of qPCR experiments monitoring the expression of *lasR* are presented in Figure 5. After the biofilm's exposure to aminated-modified polystyrene nanoparticles ($NH3^{+}$) and carboxylated-modified polystyrene nanoparticles ($COOH^{-}$), only the older biofilms (96 hr) treated with carboxylated NPs showed a significant decrease in the expression of *lasR* (p-value $_{COOH\text{-}=}$ 0.02). Reduced diffusion was also observed for carboxylated NPs in the 96 hour biofilm and is a potential relationship that should be considered more carefully in future studies.

In this study, we quantified the expression of two reference (i.e., housekeeping) genes, *ampR* and *rpsL,* by the PAO1 *ΔwspF Δpsl* P_{BAD}*pel* strain. The gene *ampR* is an ampicillin resistant gene and the *rpsL* is the gene for expression of the 30S ribosomal protein S12 which is important for maintaining translational accuracy. For the appropriate normalization of the genes expression, it is necessary that the expression of the reference genes stay constant under the experimental conditions (52). However, in this study the *rpsL* gene is not a good reference gene because in the 48 hr biofilm samples after exposure to aminated polystyrene NPs there was a significant increase (p-value $_{Exp1}$=0.01, p-value $_{Exp2}$=0.02) in *rpsL* transcript absolute copy number in both independent experimental replicates (Figure 5). While a significant increase in *rpsL* transcription was observed at 48 hr, for more mature biofilms (96 hr), there was no statistically significant difference between the normalized fold expression of *rpsL* in biofilms treated with aminated and

carboxylated polystyrene NPs and untreated biofilms. Increased expression of ribosomal subunits could increase ribosome concentrations thereby increasing total protein synthesis in the bacteria. In support of this idea, the increase in expression of the *rpsL* gene was reflected in the total protein concentration measured in the cell pellet portion of the 48 hr biofilm samples treated with aminated NPs. This is also the condition with the greatest partial confinement (Figure 3, Figure S7) and most limited particle path (Figure 4), suggesting a potential influence of cell bound proteins on movement of aminated NPs in these biofilms.

Gram-negative bacteria, like *P. aeruginosa* have a thin cell wall with a peptidoglycan layer and a lipopolysaccharide outer membrane which makes them more susceptible to NPs than Gram-positive bacteria which have a peptidoglycan layer on their surface. The negatively charged lipopolysaccharide outer membrane of *P. aeruginosa* can have attractive electrostatic interactions with the positively charge aminated NPs. For example, chitosan-based NPs, which contain amine groups, have been broadly used as drug delivery systems and display intrinsic antibacterial and antibiofilm activity due to their polycationic nature which is associated with bacterial membrane disruption (53). This disruption can cause oxidative stress in cells resulting in damage to DNA, RNA, lipids and proteins.

Aminated polystyrene nanoparticles have been found to induce reactive oxygen species (ROS) in an *in vitro* model of HeLa cells (54). In response to ROS bacteria have antioxidant defense systems. In a previous study, researchers found that *OxyR*, a transcriptional regulator that can up-regulate the expression of defensive genes in *P. aeruginosa* when the cell is in contact with hydrogen peroxide, is associated with the transcriptional regulation of *rpsL* (55). The authors hypothesized that in oxidative stress conditions *rpsL* would be under expressed based on

previous studies where protein synthesis was inhibited in response to oxidative stress by hydrogen peroxide (56). The qPCR experimental results in this study showed an increase in the expression of *rpsL* and in the intracellular/cell bound total protein concentration. Further studies are needed to elucidate the mechanisms behind this behavior in *rpsL* transcription and identify possible explanations, like for example, whether aminated particles can cause errors in bacterial translation and produce defective proteins as observed for the ribosome targeting aminoglycoside antibiotics (57,58).

These results suggest that even simple polystyrene NPs may be stressors for *P. aeruginosa* and lead to changes in the production of polysaccharides and quorum sensing signals, but the effects will depend on the variables considered in this study, NP surface charge, gene function and biofilm age, along with other environmental factors.

Further studies are needed to identify the mechanisms and processes behind the behaviors identified in this study after the PAO1 *ΔwspF Δpsl* P_{BAD}*pel* exposure to polystyrene NPs and the direct implications for biofilm architecture and metabolic efficiency. In order to identify the mechanisms that are causing the down and up regulation of the genes the system should be simplified to two or three components and systematically increased in complexity. This bottom-up approach to the biological system combined with viability assays and gene expression analysis could aid in elucidating whether the observed effects on gene transcription are due to direct interactions between NPs and bacterial cells or if these effects are induced as a cellular response due to NP interactions with other biofilm components.

CONCLUSION

The fate and transport of nanoparticles (NPs) in the environment is hard to predict due to the highly variable environmental conditions and the long list of unique properties and compositions that NPs can exhibit. When nanoparticles meet biofilms, they first deposit and accumulate in the matrix and then they diffuse through the extracellular polymeric substances (EPS) matrix if the conditions are favorable. This research highlights the importance of the biofilm matrix properties in evaluating and predicting NP transport leading to a better understanding of the natural spatial heterogeneity of the EPS, how local structural micro-domains affect the mobility of NPs in biofilms and providing a window into the complex interplay between nanoparticles, microbial transcription, and biofilm architecture.

Real biofilms are dynamic and active with responsive interchange between the microbial inhabitants and the biofilm structure, and the nanoparticle mobility will be dictated by not only the physicochemical properties of the particle but also the time and environment dependent biofilm properties. NP diffusion modes can be affected by the intrinsic variability of biofilms even when formed in similar conditions and by the same microorganism.

When nanoparticles accumulate in biofilms, their presence can be a stressor to the cells and can affect the expression of genes related to extracellular polymeric substances production and quorum sensing systems. Depending on NP surface charge, gene function and biofilm age, even simple polystyrene NPs can be stressors for bacterial cells and lead to changes in the production of polysaccharides and quorum sensing signals, which could end up affecting biofilm architecture and metabolic efficiency. And these NP-biofilm interactions are reflected in the NP transport within the biofilm.

In general, biofilms are complex matrices that, due to their intrinsic heterogeneity and dynamic and active responses to environmental changes, increase the complexity of studies related to NP accumulation and transport. It is hard to generalize the behavior of NPs in biofilms because the environmental conditions, the EPS physicochemical properties, the bacterial metabolic capabilities, and the NP properties, all play a role in the NP-biofilm interactions, which should all be taken in consideration when evaluating NP-biofilm interactions.

Supplementary Information. Additional methods details and results from Experiment 2 are included in the Supplementary Information.

CONFLICTS OF INTEREST

This research was conducted while Anne Gershenson was employed at the University of Massachusetts Amherst. The opinions expressed in this article are the authors' own and do not reflect the view of the National Institutes of Health, the Department of Health and Human Services, or the United States government.

FUNDING STATEMENT

The Massachusetts Department of Transportation Highway Division under Interagency Service Agreement NO. 87790 with the University of Massachusetts Amherst funded Joann M. Rodríguez- Suárez. The views, opinions and findings in this study are those of the authors and do not reflect MassDOT official views or policies. Dr. Rodríguez- Suárez was also partially supported by the US National Science Foundation (CBET **1452613**). This work was also supported by the University of Massachusetts Amherst Interdisciplinary Research Grant program.

Table 1: Primer sequences used in qPCR experiments.

Gene	Forward (5' → 3')	Reverse (3' → 5')	Reference
pelA	CCTTCAGCCATCCGTTCTTCT	TCGCGTACGAAGTCGACCTT	(Colvin et al., 2011)
ampR	GCGCCATCCCTTCATCG	GATGTCGACGCGGTTGTTG	
lasR	TTTCTGGGAACCGTCCATCT	GCCGAGGCTTCCTCGAA	(Mellbye & Schuster, 2014)
rpsL	GCTGTGCTCTTGCAGGTTGTG	GCAAACTATCAACCAGCTGGTG	

Table 2: Average number of aminated and carboxylated polystyrene NPs identified in a microscopy video of 6,000 frames (3 minutes) for the 48 hr and 96 hr biofilm samples. The average values are considering 3 fields of view from each sample in an area of 793 μm^2. Experiment 1 and 2 are independent experimental replicates.

Condition		48 hr biofilm	96 hr biofilm
Experiment 1	NH_3^+	36 ± 6	36 ± 33
	$COOH^-$	63 ± 25	152 ± 27
Experiment 2	NH_3^+	52 ± 20	62 ± 13
	$COOH^-$	84 ± 36	190 ± 43

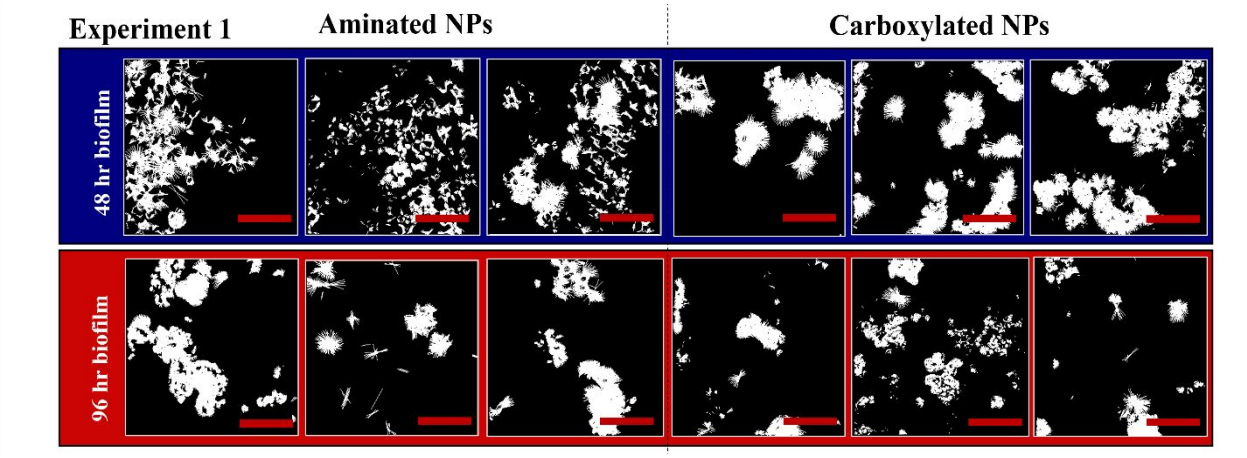

Figure 1: Connectivity maps for all three fields of view (28.2 µm x 28.2 µm) obtained by 2D-pCF analysis for the aminated and carboxylated NPs at a depth of z = 4500 ± 703 µm for the microscopy images from Experiment 1. Each row shows a field of view analyzed for the 48 hr biofilm samples (blue) and the 96 hr biofilms samples (red). The scale bar (red) in each map is 10 µm.

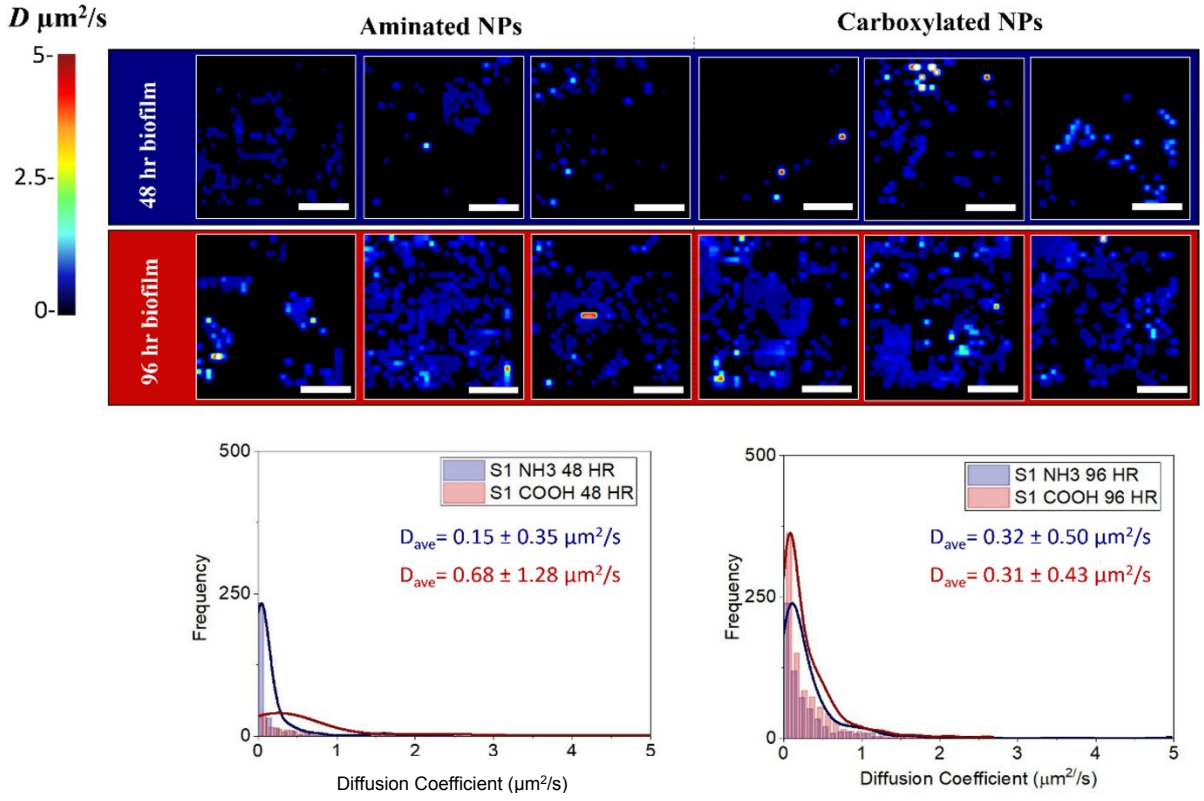

Figure 2: Visual maps and diffusion coefficient histograms for the aminated and carboxylated polystyrene nanoparticles diffusing at a depth of z = 4500 ± 703 µm. The diffusion coefficients were obtained from the iMSD analysis of the microscopy images from Experiment 1. The bars are histograms with bins sizes of 0.1 µm^2 /s. The lines are kernel (Scott) probability density estimates of the diffusion coefficient (D) distributions. Each row shows the maps from the 48 hr and 96 hr biofilm samples. The D heatmap color scale goes from black to red. The red areas are those with higher D values (faster diffusion) and the blacker areas are the ones with the lower D values (slower diffusion). The color-coded values in the distribution graphs are average values of the D distributions taking into consideration all 3 fields of view analyzed. The scale bar (white) in each map is 10 µm.

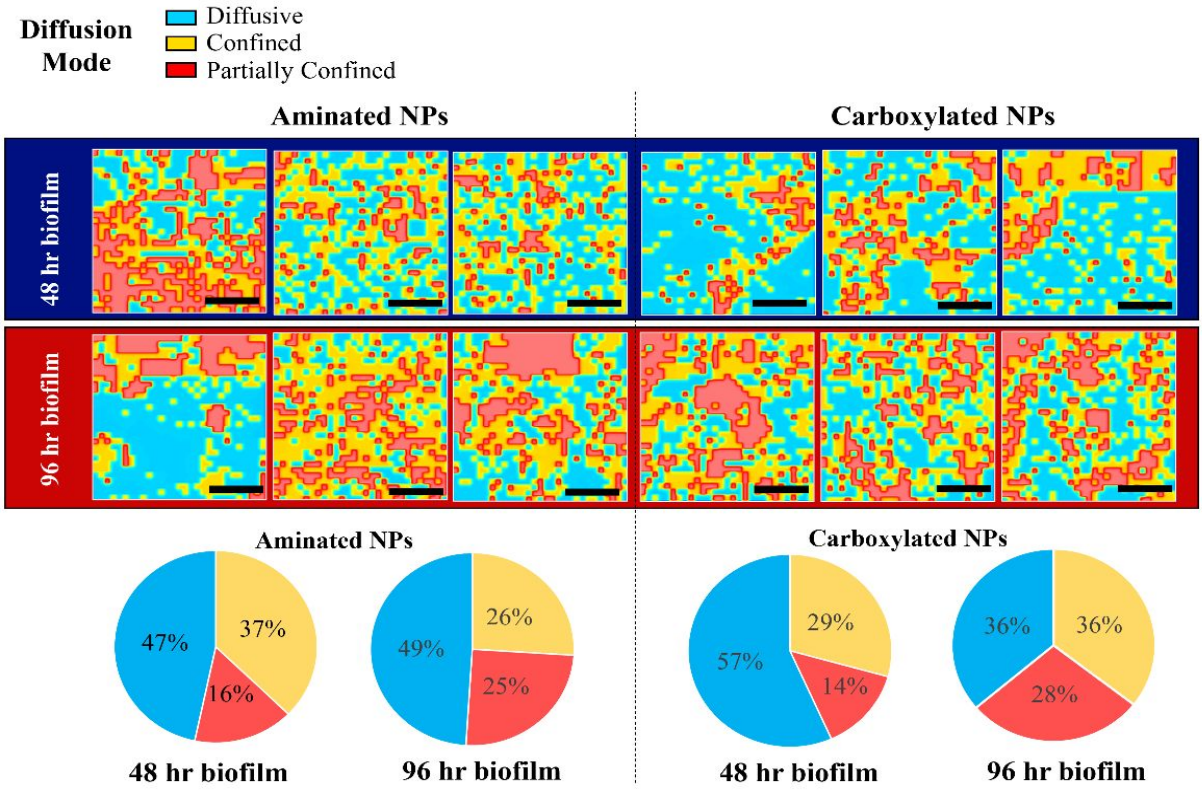

Figure 3: Maps of diffusion modes, freely diffusive (blue), confined (yellow) and partially confined (red). Each row shows each field of view analyzed for the 48 hr biofilms and the 96 hr biofilm amples in Experiment 1. The pie charts represent the average percentage (for all three fields of view analyzed) showing free diffusion (blue), confined (yellow) or partially confined (red) areas for each type of NP. The scale bar (black) in each map is 10 μm and the z depth was 4500 ± 703 μm.

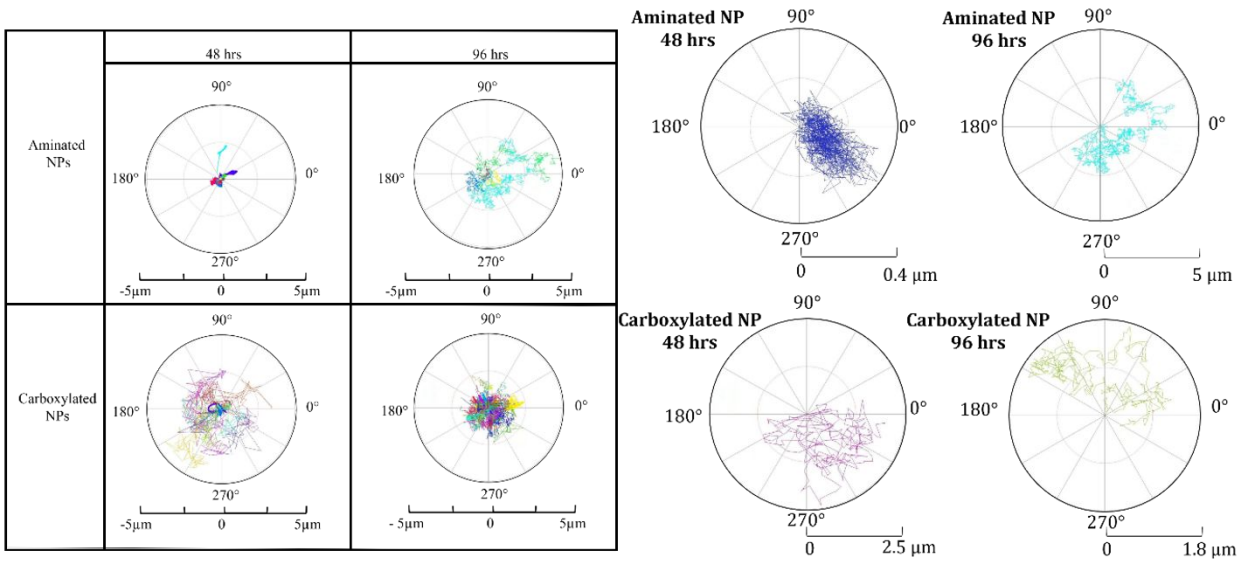

Figure 4: Polar graphs of individual tracks (from SPT) for all three fields of view from Experiment 1 biofilms at a z depth of 4500 ± 703 μm. Each track has an assigned color that represents a single nanoparticle with the origin representing the nanoparticle initial position. All the nanoparticle tracks for the three fields of view are presented in the polar graph for each nanoparticle considered. The polar graphs on the right represent a zoom in of individual particle tracks for aminated and carboxylated NPs in the biofilm samples.

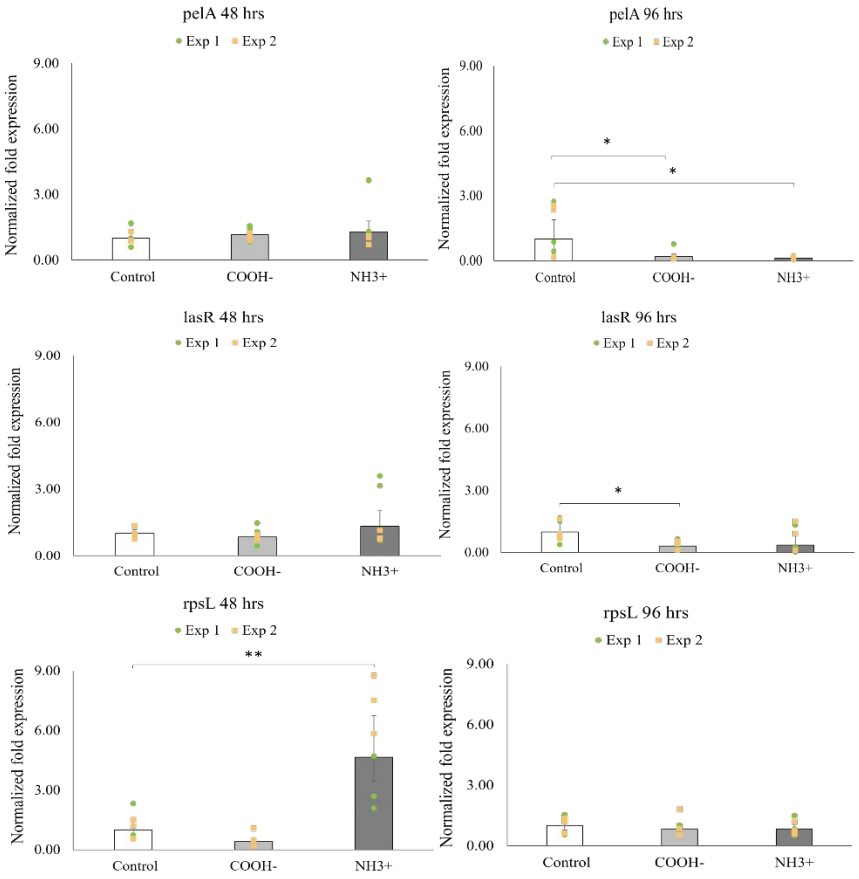

Figure 5: Normalized fold expression of *pelA, lasR* and *rpsL* transcription by PAO1 ΔwspF Δpsl P_{BAD}pel bacterial strain for unexposed biofilms (Control) and NP treated biofilm samples (aminated polystyrene ($NH3^+$) and carboxylated polystyrene ($COOH^-$)). The values correspond to two independent experiments and triplicate biological samples for each experiment for each condition (green and yellow symbols indicate the two independent experiments). The qPCR results were normalized to the results for the reference gene *ampR*. The error bars represent the standard error of the mean of 6 biological samples (3 from each experimental replicate). Asterisks indicate statistical significance, * for $p \leq 0.05$ and ** for $p \leq 0.01$.

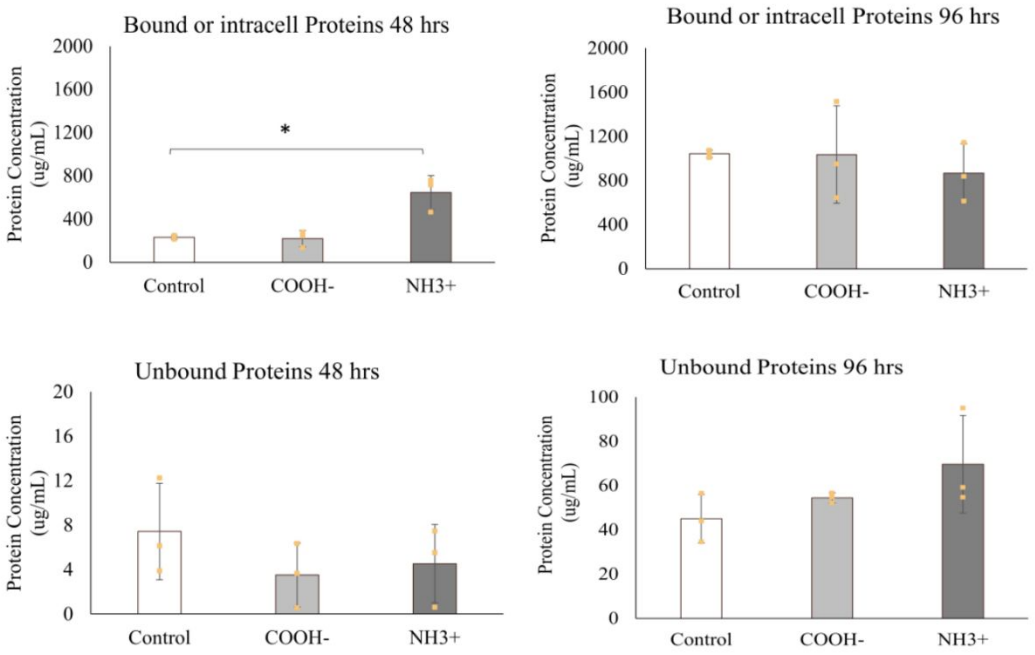

Figure 6: Total protein concentration measured in the biofilm samples. The concentration of intracellular proteins (protein within the cell) and protein bound to the bacteria were measured for the cell pellet collected from the biofilm samples while the unbound proteins were measured in the sample supernatant using the Qubit protein assay kit. The values correspond to triplicates of biological samples under each condition for two independent experiments. The error bars represent the standard deviation of 6 biological samples (3 from each experimental replicate). Asterisks indicate statistical significance, * for $p < 0.05$ and ** for $p < 0.01$.

REFERENCES

1. Keller AA, Vosti W, Wang H, Lazareva A. Release of engineered nanomaterials from personal care products throughout their life cycle. J Nanoparticle Res [Internet]. 2014 Jul [cited 2023 Feb 27];16(7):2489. Available from: http://link.springer.com/10.1007/s11051-014-2489-9

2. Nomura T, Fujisawa E, Itoh S, Konishi Y. Comparison of the cytotoxic effect of polystyrene latex nanoparticles on planktonic cells and bacterial biofilms. J Nanoparticle Res [Internet]. 2016 Jun [cited 2023 Feb 27];18(6):157. Available from: http://link.springer.com/10.1007/s11051-016-3471-5

3. Janković NZ, Plata DL. Engineered nanomaterials in the context of global element cycles. Environ Sci Nano [Internet]. 2019 [cited 2023 Mar 4];6(9):2697–711. Available from: http://xlink.rsc.org/?DOI=C9EN00322C

4. Nikalje AP. Nanotechnology and its Applications in Medicine. Med Chem [Internet]. 2015 [cited 2023 Mar 4];5(2). Available from: https://www.omicsonline.org/open-access/nanotechnology-and-its-applications-in-medicine-2161-0444-1000247.php?aid=41535

5. Joo SH, Aggarwal S. Factors impacting the interactions of engineered nanoparticles with bacterial cells and biofilms: Mechanistic insights and state of knowledge. J Environ Manage [Internet]. 2018 Nov [cited 2023 Feb 27];225:62–74. Available from: https://linkinghub.elsevier.com/retrieve/pii/S0301479718308478

6. Koelmans AA, Besseling E, Shim WJ. Nanoplastics in the Aquatic Environment. Critical Review. In: Bergmann M, Gutow L, Klages M, editors. Marine Anthropogenic Litter [Internet]. Cham: Springer International Publishing; 2015 [cited 2023 Feb 27]. p. 325–40. Available from: http://link.springer.com/10.1007/978-3-319-16510-3_12

7. Miao L, Guo S, Wu J, Adyel TM, Liu Z, Liu S, et al. Polystyrene nanoplastics change the functional traits of biofilm communities in freshwater environment revealed by GeoChip 5.0. J Hazard Mater [Internet]. 2022 Feb [cited 2023 Feb 27];423:127117. Available from: https://linkinghub.elsevier.com/retrieve/pii/S0304389421020859

8. Phuc LTM, Taniguchi A. Polystyrene Nanoparticles Induce Apoptosis or Necrosis With or Without Epidermal Growth Factor. J Nanosci Nanotechnol [Internet]. 2019 Aug 1 [cited 2023 Mar 2];19(8):4812–7. Available from: https://www.ingentaconnect.com/content/10.1166/jnn.2019.16347

9. Arora S, Rajwade JM, Paknikar KM. Nanotoxicology and in vitro studies: The need of the hour. Toxicol Appl Pharmacol [Internet]. 2012 Jan [cited 2023 Feb 27];258(2):151–65. Available from: https://linkinghub.elsevier.com/retrieve/pii/S0041008X11004467

10. Ferrari M. Cancer nanotechnology: opportunities and challenges. Nat Rev Cancer [Internet]. 2005 Mar 1 [cited 2023 Feb 27];5(3):161–71. Available from: http://www.nature.com/articles/nrc1566

11. Joshi AS, Singh P, Mijakovic I. Interactions of Gold and Silver Nanoparticles with Bacterial Biofilms: Molecular Interactions behind Inhibition and Resistance. Int J Mol Sci [Internet]. 2020 Oct 16 [cited 2023 Feb 27];21(20):7658. Available from: https://www.mdpi.com/1422-0067/21/20/7658

12. Peulen TO, Wilkinson KJ. Diffusion of Nanoparticles in a Biofilm. Environ Sci Technol [Internet]. 2011 Apr 15 [cited 2023 Feb 27];45(8):3367–73. Available from: https://pubs.acs.org/doi/10.1021/es103450g

13. Remis JP, Costerton JW, Auer M. Biofilms: structures that may facilitate cell–cell interactions. ISME J [Internet]. 2010 Sep [cited 2023 Feb 27];4(9):1085–7. Available from: http://www.nature.com/articles/ismej2010105

14. Birjiniuk A, Billings N, Nance E, Hanes J, Ribbeck K, Doyle PS. Single particle tracking reveals spatial and dynamic organization of the *Escherichia coli* biofilm matrix. New J Phys [Internet]. 2014 Aug 27 [cited 2023 Feb 27];16(8):085014. Available from: https://iopscience.iop.org/article/10.1088/1367-2630/16/8/085014

15. Rodríguez-Suárez JM, Butler CS, Gershenson A, Lau BLT. Heterogeneous Diffusion of Polystyrene Nanoparticles through an Alginate Matrix: The Role of Cross-linking and Particle Size. Environ Sci Technol [Internet]. 2020 Apr 21 [cited 2023 Feb 27];54(8):5159–66. Available from: https://pubs.acs.org/doi/10.1021/acs.est.9b06113

16. Chew SC, Rice SA, Kjelleberg S, Yang L. In Situ Mapping of the Mechanical Properties of Biofilms by Particle-tracking Microrheology. J Vis Exp [Internet]. 2015 Dec 4 [cited 2023 Feb 27];(106):53093. Available from: https://www.jove.com/t/53093/in-situ-mapping-of-the-mechanical-properties-of-biofilms-by-particle--tracking-microrheology

17. Ikuma K, Decho AW, Lau BLT. When nanoparticles meet biofilmsâ€"interactions guiding the environmental fate and accumulation of nanoparticles. Front Microbiol [Internet]. 2015 Jun 16 [cited 2023 Feb 27];6. Available from: http://journal.frontiersin.org/Article/10.3389/fmicb.2015.00591/abstract

18. Vitale S, Rampazzo E, Hiebner D, Devlin H, Quinn L, Prodi L, et al. Interaction between Engineered Pluronic Silica Nanoparticles and Bacterial Biofilms: Elucidating the Role of Nanoparticle Surface Chemistry and EPS Matrix. ACS Appl Mater Interfaces [Internet]. 2022 Aug 3 [cited 2023 Feb 27];14(30):34502–12. Available from: https://pubs.acs.org/doi/10.1021/acsami.2c10347

19. Ikuma K, Madden AS, Decho AW, Lau BLT. Deposition of nanoparticles onto polysaccharide-coated surfaces: implications for nanoparticle–biofilm interactions. Env Sci Nano [Internet].

2014 [cited 2023 Feb 27];1(2):117–22. Available from: http://xlink.rsc.org/?DOI=C3EN00075C

20. Chompoosor A, Saha K, Ghosh PS, Macarthy DJ, Miranda OR, Zhu ZJ, et al. The Role of Surface Functionality on Acute Cytotoxicity, ROS Generation and DNA Damage by Cationic Gold Nanoparticles. Small [Internet]. 2010 Oct 18 [cited 2023 Feb 27];6(20):2246–9. Available from: https://onlinelibrary.wiley.com/doi/10.1002/smll.201000463

21. Li Y, Zhang W, Niu J, Chen Y. Surface-Coating-Dependent Dissolution, Aggregation, and Reactive Oxygen Species (ROS) Generation of Silver Nanoparticles under Different Irradiation Conditions. Environ Sci Technol [Internet]. 2013 Sep 4 [cited 2023 Feb 27];130904083900006. Available from: https://pubs.acs.org/doi/abs/10.1021/es400945v

22. Erdim E, Badireddy AR, Wiesner MR. Characterizing reactive oxygen generation and bacterial inactivation by a zerovalent iron-fullerene nano-composite device at neutral pH under UV-A illumination. J Hazard Mater [Internet]. 2015 Feb [cited 2023 Mar 4];283:80–8. Available from: https://linkinghub.elsevier.com/retrieve/pii/S0304389414007122

23. Patil MA, Parikh PA. Investigation on Likely Effects of Ag, TiO2, and ZnO Nanoparticles on Sewage Treatment. Bull Environ Contam Toxicol [Internet]. 2014 Jan [cited 2023 Mar 4];92(1):109–14. Available from: http://link.springer.com/10.1007/s00128-013-1141-1

24. von Moos N, Slaveykova VI. Oxidative stress induced by inorganic nanoparticles in bacteria and aquatic microalgae – state of the art and knowledge gaps. Nanotoxicology [Internet]. 2014 Sep [cited 2023 Mar 4];8(6):605–30. Available from: http://www.tandfonline.com/doi/full/10.3109/17435390.2013.809810

25. Wang Z, Hessler CM, Xue Z, Seo Y. The role of extracellular polymeric substances on the sorption of natural organic matter. Water Res [Internet]. 2012 Mar [cited 2023 Mar 4];46(4):1052–60. Available from: https://linkinghub.elsevier.com/retrieve/pii/S004313541100769X

26. Ševců A, El-Temsah YS, Filip J, Joner EJ, Bobčíková K, Černík M. Zero-valent iron particles for PCB degradation and an evaluation of their effects on bacteria, plants, and soil organisms. Environ Sci Pollut Res [Internet]. 2017 Sep [cited 2023 Mar 4];24(26):21191–202. Available from: http://link.springer.com/10.1007/s11356-017-9699-5

27. García-Lara B, Saucedo-Mora MÁ, Roldán-Sánchez JA, Pérez-Eretza B, Ramasamy M, Lee J, et al. Inhibition of quorum-sensing-dependent virulence factors and biofilm formation of clinical and environmental *Pseudomonas aeruginosa* strains by ZnO nanoparticles. Lett Appl Microbiol [Internet]. 2015 Sep [cited 2023 Feb 27];61(3):299–305. Available from: https://academic.oup.com/lambio/article/61/3/299/6699748

28. Mellbye B, Schuster M. Physiological Framework for the Regulation of Quorum Sensing-Dependent Public Goods in Pseudomonas aeruginosa. J Bacteriol [Internet]. 2014 Mar 15

[cited 2023 Feb 27];196(6):1155–64. Available from: https://journals.asm.org/doi/10.1128/JB.01223-13

29. Kassinger SJ, van Hoek ML. Biofilm architecture: An emerging synthetic biology target. Synth Syst Biotechnol [Internet]. 2020 Mar [cited 2023 Feb 27];5(1):1–10. Available from: https://linkinghub.elsevier.com/retrieve/pii/S2405805X20300016

30. Jennings LK, Storek KM, Ledvina HE, Coulon C, Marmont LS, Sadovskaya I, et al. Pel is a cationic exopolysaccharide that cross-links extracellular DNA in the *Pseudomonas aeruginosa* biofilm matrix. Proc Natl Acad Sci [Internet]. 2015 Sep 8 [cited 2023 Feb 27];112(36):11353–8. Available from: https://pnas.org/doi/full/10.1073/pnas.1503058112

31. Allesen-Holm M, Barken KB, Yang L, Klausen M, Webb JS, Kjelleberg S, et al. A characterization of DNA release in Pseudomonas aeruginosa cultures and biofilms. Mol Microbiol [Internet]. 2006 Feb [cited 2023 Feb 27];59(4):1114–28. Available from: https://onlinelibrary.wiley.com/doi/10.1111/j.1365-2958.2005.05008.x

32. Colvin KM, Gordon VD, Murakami K, Borlee BR, Wozniak DJ, Wong GCL, et al. The Pel Polysaccharide Can Serve a Structural and Protective Role in the Biofilm Matrix of Pseudomonas aeruginosa. Ausubel FM, editor. PLoS Pathog [Internet]. 2011 Jan 27 [cited 2023 Mar 4];7(1):e1001264. Available from: https://dx.plos.org/10.1371/journal.ppat.1001264

33. Jaqaman K, Loerke D, Mettlen M, Kuwata H, Grinstein S, Schmid SL, et al. Robust single-particle tracking in live-cell time-lapse sequences. Nat Methods [Internet]. 2008 Aug [cited 2023 Feb 27];5(8):695–702. Available from: http://www.nature.com/articles/nmeth.1237

34. Malacrida L, Rao E, Gratton E. Comparison between iMSD and 2D-pCF analysis for molecular motion studies on in vivo cells: The case of the epidermal growth factor receptor. Methods [Internet]. 2018 May [cited 2023 Feb 27];140–141:74–84. Available from: https://linkinghub.elsevier.com/retrieve/pii/S1046202317303614

35. Colvin KM, Irie Y, Tart CS, Urbano R, Whitney JC, Ryder C, et al. The Pel and Psl polysaccharides provide Pseudomonas aeruginosa structural redundancy within the biofilm matrix: Polysaccharides of the P. aeruginosa biofilm matrix. Environ Microbiol [Internet]. 2012 Aug [cited 2023 Feb 27];14(8):1913–28. Available from: https://onlinelibrary.wiley.com/doi/10.1111/j.1462-2920.2011.02657.x

36. Taylor SC, Nadeau K, Abbasi M, Lachance C, Nguyen M, Fenrich J. The Ultimate qPCR Experiment: Producing Publication Quality, Reproducible Data the First Time. Trends Biotechnol [Internet]. 2019 Jul [cited 2023 Mar 4];37(7):761–74. Available from: https://linkinghub.elsevier.com/retrieve/pii/S0167779918303421

37. Stewart PS. A review of experimental measurements of effective diffusive permeabilities and effective diffusion coefficients in biofilms. Biotechnol Bioeng [Internet]. 1998 Aug 5

[cited 2023 Feb 27];59(3):261–72. Available from: https://onlinelibrary.wiley.com/doi/10.1002/(SICI)1097-0290(19980805)59:3<261::AID-BIT1>3.0.CO;2-9

38. Nevius BA, Chen YP, Ferry JL, Decho AW. Surface-functionalization effects on uptake of fluorescent polystyrene nanoparticles by model biofilms. Ecotoxicology [Internet]. 2012 Nov [cited 2023 Jul 21];21(8):2205–13. Available from: http://link.springer.com/10.1007/s10646-012-0975-3

39. Marmont LS, Whitfield GB, Rich JD, Yip P, Giesbrecht LB, Stremick CA, et al. PelA and PelB proteins form a modification and secretion complex essential for Pel polysaccharide-dependent biofilm formation in Pseudomonas aeruginosa. J Biol Chem [Internet]. 2017 Nov [cited 2023 Feb 27];292(47):19411–22. Available from: https://linkinghub.elsevier.com/retrieve/pii/S0021925820329094

40. Zając M, Kotyńska J, Zambrowski G, Breczko J, Deptuła P, Cieśluk M, et al. Exposure to polystyrene nanoparticles leads to changes in the zeta potential of bacterial cells. Sci Rep [Internet]. 2023 Jun 12 [cited 2023 Jul 21];13(1):9552. Available from: https://www.nature.com/articles/s41598-023-36603-5

41. Renner LD, Weibel DB. Physicochemical regulation of biofilm formation. MRS Bull [Internet]. 2011 May [cited 2023 Jul 21];36(5):347–55. Available from: http://link.springer.com/10.1557/mrs.2011.65

42. Huangfu X, Xu Y, Liu C, He Q, Ma J, Ma C, et al. A review on the interactions between engineered nanoparticles with extracellular and intracellular polymeric substances from wastewater treatment aggregates. Chemosphere [Internet]. 2019 Mar [cited 2023 Jul 21];219:766–83. Available from: https://linkinghub.elsevier.com/retrieve/pii/S004565351832366X

43. Flemming HC, Wingender J. The biofilm matrix. Nat Rev Microbiol [Internet]. 2010 Sep [cited 2023 Mar 27];8(9):623–33. Available from: http://www.nature.com/articles/nrmicro2415

44. Habimana O, Semião AJC, Casey E. The role of cell-surface interactions in bacterial initial adhesion and consequent biofilm formation on nanofiltration/reverse osmosis membranes. J Membr Sci [Internet]. 2014 Mar [cited 2023 Jul 21];454:82–96. Available from: https://linkinghub.elsevier.com/retrieve/pii/S0376738813009393

45. Benigar E, Zupančič Valant A, Dogsa I, Sretenovic S, Stopar D, Jamnik A, et al. Structure and Dynamics of a Model Polymer Mixture Mimicking a Levan-Based Bacterial Biofilm of *Bacillus subtilis*. Langmuir [Internet]. 2016 Aug 16 [cited 2023 Feb 27];32(32):8182–94. Available from: https://pubs.acs.org/doi/10.1021/acs.langmuir.6b02041

46. Sprakel J, van der Gucht J, Cohen Stuart MA, Besseling NAM. Rouse Dynamics of Colloids Bound to Polymer Networks. Phys Rev Lett [Internet]. 2007 Nov 15 [cited 2023 Feb 27];99(20):208301. Available from: https://link.aps.org/doi/10.1103/PhysRevLett.99.208301

47. Sankaran J, Tan NJHJ, But KP, Cohen Y, Rice SA, Wohland T. Single microcolony diffusion analysis in Pseudomonas aeruginosa biofilms. Npj Biofilms Microbiomes [Internet]. 2019 Nov 8 [cited 2023 Feb 27];5(1):35. Available from: https://www.nature.com/articles/s41522-019-0107-4

48. Witten J, Ribbeck K. The particle in the spider's web: transport through biological hydrogels. Nanoscale [Internet]. 2017 [cited 2023 Feb 27];9(24):8080–95. Available from: http://xlink.rsc.org/?DOI=C6NR09736G

49. Vater SM, Weiße S, Maleschlijski S, Lotz C, Koschitzki F, Schwartz T, et al. Swimming Behavior of Pseudomonas aeruginosa Studied by Holographic 3D Tracking. van Veen HW, editor. PLoS ONE [Internet]. 2014 Jan 31 [cited 2023 Feb 27];9(1):e87765. Available from: https://dx.plos.org/10.1371/journal.pone.0087765

50. Friedman L, Kolter R. Genes involved in matrix formation in Pseudomonas aeruginosa PA14 biofilms: Matrix formation in P. aeruginosa PA14 biofilms. Mol Microbiol [Internet]. 2003 Dec 16 [cited 2023 Feb 27];51(3):675–90. Available from: http://doi.wiley.com/10.1046/j.1365-2958.2003.03877.x

51. Colvin KM, Alnabelseya N, Baker P, Whitney JC, Howell PL, Parsek MR. PelA Deacetylase Activity Is Required for Pel Polysaccharide Synthesis in Pseudomonas aeruginosa. J Bacteriol [Internet]. 2013 May 15 [cited 2023 Mar 4];195(10):2329–39. Available from: https://journals.asm.org/doi/10.1128/JB.02150-12

52. Derveaux S, Vandesompele J, Hellemans J. How to do successful gene expression analysis using real-time PCR. Methods [Internet]. 2010 Apr [cited 2023 Feb 27];50(4):227–30. Available from: https://linkinghub.elsevier.com/retrieve/pii/S1046202309002461

53. Ilk S, Sağlam N, Özgen M, Korkusuz F. Chitosan nanoparticles enhances the anti-quorum sensing activity of kaempferol. Int J Biol Macromol [Internet]. 2017 Jan [cited 2023 Feb 27];94:653–62. Available from: https://linkinghub.elsevier.com/retrieve/pii/S0141813016320876

54. Sharma A, Gorey B, Casey A. *In vitro* comparative cytotoxicity study of aminated polystyrene, zinc oxide and silver nanoparticles on a cervical cancer cell line. Drug Chem Toxicol [Internet]. 2019 Jan 2 [cited 2023 Feb 27];42(1):9–23. Available from: https://www.tandfonline.com/doi/full/10.1080/01480545.2018.1424181

55. Wei Q, Le Minh PN, Dötsch A, Hildebrand F, Panmanee W, Elfarash A, et al. Global regulation of gene expression by OxyR in an important human opportunistic pathogen.

Nucleic Acids Res [Internet]. 2012 May [cited 2023 Feb 27];40(10):4320–33. Available from: https://academic.oup.com/nar/article-lookup/doi/10.1093/nar/gks017

56. Palma M, DeLuca D, Worgall S, Quadri LEN. Transcriptome Analysis of the Response of *Pseudomonas aeruginosa* to Hydrogen Peroxide. J Bacteriol [Internet]. 2004 Jan [cited 2023 Feb 27];186(1):248–52. Available from: https://journals.asm.org/doi/10.1128/JB.186.1.248-252.2004

57. Mingeot-Leclercq MP, Glupczynski Y, Tulkens PM. Aminoglycosides: Activity and Resistance. Antimicrob Agents Chemother [Internet]. 1999 Apr [cited 2023 Feb 27];43(4):727–37. Available from: https://journals.asm.org/doi/10.1128/AAC.43.4.727

58. Pelchovich G, Schreiber R, Zhuravlev A, Gophna U. The contribution of common rpsL mutations in Escherichia coli to sensitivity to ribosome targeting antibiotics. Int J Med Microbiol [Internet]. 2013 Dec [cited 2023 Feb 27];303(8):558–62. Available from: https://linkinghub.elsevier.com/retrieve/pii/S1438422113001021